Binding of Nucleotides by the Mitochondrial ADP/ATP Carrier as Studied by ^{1}H Nuclear Magnetic Resonance Spectroscopy†

Thomas Huber, Martin Klingenberg, and Klaus Beyer*

Institute of Physical Biochemistry, University of Munich, Schillerstrasse 44, 80336 München, Germany

Received June 16, 1998; Revised Manuscript Received September 30, 1998

ABSTRACT: Nucleotide binding to the cytosolic binding site of the mitochondrial ADP/ATP carrier (AAC) was studied by ^{1}H-nuclear magnetic resonance spectroscopy. Binding (as opposed to translocation) could be identified as a result of the rapid ligand on/off kinetics, using the cytosolic side specific inhibitor carboxyatractyloside (CAT) for the distinction from nonspecific interactions. The off rate constant of the nonhydrolyzable ATP analogue AMP−PCP was more than 3 orders of magnitude larger than the transport rate. The nucleotides adopt an anti conformation in the carrier binding site as shown by measurements of the transferred nuclear overhauser effect (TRNOE). A thermal transition around 14 °C that had been previously detected in transport studies [Klingenberg, M., Grebe, K., and Appel, M. (1982) *Eur. J. Biochem. 126*, 263−269] was reflected by the inhibitor sensitive line broadening, indicating that this transition also affects nucleotide binding. Nucleotide monophosphates were employed to study the relation between nucleotide structure and affinity, using selective excitation, sample spinning with digital suppression of spinning sidebands, and line shape simulation. The binding of purines depends on the distribution of the electrical potential and on the position of ring substituents, while pyrimidines are barely recognized at all by the AAC. It is also shown that the photocleavable "caged" derivatives are more tightly bound than the original nucleotides. A two step model of carrier catalysis will be discussed on the basis of these results.

The ADP/ATP carrier (AAC)[1] is the paradigm member of a family of mitochondrial inner membrane transport proteins (*1*, *2*). These proteins share a number features such as a homodimeric functional unit, a molecular weight of ∼30−35 kDa/monomer, and a triplicate primary structure (*1*). Although in the AAC for the first time partial steps of the translocation, that is, the binding site reorientation, could be detected on the molecular level, little is known about the binding site and the structure of the translocation channel. Therefore also key steps of substrate recognition and gating are still poorly understood.

The transport by the AAC employs an exchange which has been characterized as a single binding site gated pore mechanism (*3*). The protein can be arrested by the highly specific transport inhibitors carboxyatractylate (CAT), atractylate (ATR), and bongkrekic acid (BKA) in its reciprocal conformational states where the binding center is open to the external or internal face of the membrane, respectively. In mitochondria the inhibitor CAT and ATR binds only from the cytosolic ("c") side and BKA from the matrix ("m") side of the inner membrane. It is assumed that these tightly binding inhibitors drive the carrier into an "abortive ground state", in contrast to the translocated nucleotides.

Equilibrium nucleotide binding to the AAC was measured so far only on bovine heart mitochondria by conventional methods (*4*). Nuclear magnetic resonance offers some advantages for a study of transient protein−ligand interaction, provided that the lifetime of the bound ligand state is smaller than the spin lattice relaxation time of the observed ligand nuclei. The dissociation kinetics of the substrate may then be obtained by measuring the relaxation times (or equivalently the line broadenings) of substrate nuclei. In the present study we have measured the line broadening of purine and pyrimidine ring proton signals on binding to mitochondria. The inhibitors were employed in order to discriminate binding to the AAC from binding to other proteins or to the membrane surface. The inhibitor sensitive line broadening revealed carrier binding of purine nucleotides other than ATP and ADP despite their small or negligible transport competence. Intramolecular cross relaxation (TRNOE) indicates that the nucleotides interact in an anti conformation. The rapid on/off exchange of the nucleotides as observed by NMR not only affords an insight into the binding selectivity but also lends itself to a direct comparison with earlier work on the transport activity. The temperature dependence of the line broadening and of the transport activity as determined previously (*5*) suggests that the AAC undergoes a structural transition around 14 °C. Moreover, the sensitivity of nucleotide binding to changes in ionic strength was directly demonstrated here and will be discussed with reference to earlier work (*6*, *7*). The present results will be integrated into a model which entails weak nucleotide binding upon recognition and specific gating by the transport competent nucleotides.

† This work was supported by a grant from the Deutschen Forschungsgemeinschaft (SFB 266, TP B12).

* To whom correspondence should be addressed.

[1] Abbreviations: AAC, ADP/ATP carrier protein; AMP−PCP, β,γ-methyleneadenosine-5′-triphosphate; AMP−PNP, β,γ-imidoadenosine-5′-triphosphate; ATR, atractylate; BKA, bongkrekic acid; CAT, carboxyatractylate; DSS, 3-(trimethylsilyl)-1-propanesulfonic acid.

10.1021/bi981431l CCC: $18.00
Published on Web 12/19/1998

MATERIALS AND METHODS

Chemicals. Nucleotides and nucleotide derivatives were purchased from Sigma and from Boehringer, Mannheim at the highest purity available. Deuterium oxide (99.8% deuterium enrichment) was from Merck, Darmstadt. Polystyrene beads (XAD-2) were from Fluka and phospholipids from Avanti Polar Lipids, Inc., Alabaster, AL.

Preparative Procedures. The concentration of the inhibitor BKA was determined photometrically at 263 nm using an extinction coefficient of 40.6 mM^{-1} cm^{-1} (*8*). Bovine heart mitochondria were prepared essentially as described by Blair (*9*) in 250 mM sucrose and 20 mM Tris-buffer, pH 7.4. The final suspension (typically 45−60 mg/mL of mitochondrial protein) was diluted 8-fold with a buffer containing 50 mM potassium phosphate in D_2O at pD 7.0. After incubation for 30 min at room temperature the suspension was centrifuged at 18000*g* at 4 °C. The pellet was resuspended in a 3-fold buffer volume (150 mM KCl and 20 mM potassium phosphate in D_2O at pD 7.4). The replacement of sucrose and H_2O by KCl and D_2O was necessary in order to avoid dynamic range problems when recording ^1H NMR spectra in the mitochondrial suspensions.

NMR Spectroscopy. ^1H and ^{31}P NMR spectra of nucleotides in mitochondrial suspensions were obtained with a Varian VXR-400 S spectrometer operating at a proton frequency of 400 MHz. The line broadenings of purine and pyrimidine ring proton signals were analyzed to establish the interaction of the nucleotides with the mitochondrial ADP/ATP carrier protein. The spectral region of interest, for example, the chemical shift range from 7.0 to 8.0 ppm which covers the aromatic ring proton signals (H_2, H_8 of the purines and H_5, H_6 of the pyrimidines), was excited using a band selective ("tophat") shaped pulse (*10*). The latter spectral region is well-separated from any other resolved ^1H signal and from the broad signal background of the mitochondria. The width at half-height was obtained by fitting Lorentzian lines to the observed signals, using the carrier specific inhibitors for the discrimination of specific carrier binding. Sample spinning was routinely applied, and the spinning sidebands were removed by appropriate scaling and intersubtraction of the spectra (see Figure 1). This procedure led to considerable improvements of the statistical significance of the line width determinations (as compared to line broadening measurements without sample spinning), making experiments at mitochondrial densities as low as 8 mg of mitochondrial protein per milliliter feasible. Digital signal processing (typically 20-fold oversampling combined with a digital filter provided with the VNMR 5.1 software) was applied to suppress quantization noise. The ^1H spectra of ATP alone and of a mitochondrial suspension containing 1 mM ATP and the improvements achieved by sample spinning and spectral intersubtraction are summarized in Figure 1.

RESULTS

Nucleotide Binding and Inhibitor Competition. The interaction of nucleotides and nucleotide analogues with the mitochondrial ADP/ATP carrier was studied by ^1H NMR spectroscopy in suspensions of isolated beef heart mitochondria. Dynamic range problems were avoided by routinely replacing the standard sucrose medium with 150 mM KCl in D_2O, except for experiments where a systematic variation

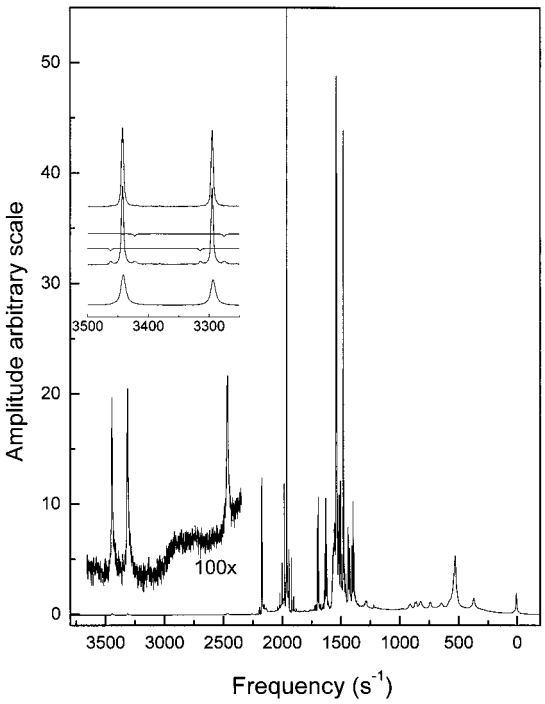

FIGURE 1: ^1H NMR spectra of bovine heart mitochondria (20 mg/mL of mitochondrial protein) in the presence of 1 mM ATP. The downfield ATP signals are 100 times vertically expanded. Removal of spinning sidebands (upper part of the inset) is demonstrated using a separate sample containing CAT preloaded mitochondria and 5 mM AMP (from bottom to top): spectrum without sample spinning; spectrum with sample spinning; matching spectra obtained by digital scaling and shifting of the center band of the spinning spectrum; sum of the spectrum obtained with sample spinning and of the two matching spectra.

of the ionic stength was desired (see below). A band selective excitation scheme was used in order to reduce the amplitude of residual water or sucrose ^1H signals. Presaturation of the residual water signal was avoided or performed with low power in order to circumvent partial saturation of the nucleotide signals by spin diffusion and direct cross relaxation (see Methods).

Transient nucleotide binding in the "c"-state of the AAC was demonstrated by inhibitor competition. Mitochondria (8 mg of mitochondrial protein) were titrated with the inhibitor CAT at 18 °C in the presence of the substrate analogue AMP−PCP, and the line widths of the nucleotide H8 and H2 signals were monitored. Competitive substrate displacement by the inhibitor results in line narrowing of the purine ^1H signals (Figure 2).The preincubation with the nucleotide facilitates the redistribution of the binding sites, rendering all accessible to CAT (*11*). The titration then yields an estimate of the total number of binding sites, assuming a 1:1 inhibitor−substrate relation. Approximately 1.2 nmol of binding sites per milligram of mitochondrial protein was obtained (Figure 2), in agreement with previous determinations using radioactive analogues (*12*, *13*). This binding ratio could also be estimated from a titration with the inhibitor BKA, although an accurate equivalence point was not available (*14*). An analogous result was obtained by titration with the less tightly binding inhibitor atractylate (ATR; see insert in Figure 2). It may be noted that there is an initial lagging phase in the ATR titration, that is, up to an addition of one-third of the ATR necessary to reach the end point the broadening changes with a smaller slope. Using ATR

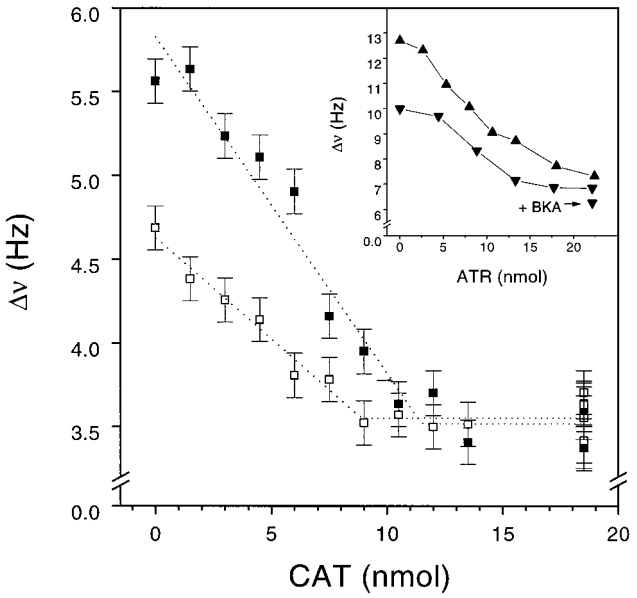

FIGURE 2: Titration of bovine heart mitochondria (8 mg of mitochondrial protein per milliliter in 150 mM KCl buffer in D_2O, pD 7.4) in the presence of 5 mM AMP−PCP with the inhibitor CAT: closed symbols, H2; open symbols, H8. The line widths were corrected for sample inhomogeneities by comparison with the ^1H signal of internal DSS (1 mg/mL). The error therefore mainly represents the uncertainty in line width determination. The regression lines were obtained by least-squares fitting according to $^1/_2(p_1 - np_2 + |p_1 - np_2|) + p_3$, with n denoting the amount of added CAT, p_1, p_2, and p_3 the independent fitting parameters, and the vertical bars absolute values. (Insert) Titration with the inhibitor ATR (8 mg of mitochondrial protein per milliliter, same buffer as above, pD 6.92): AMP−PCP concentration, 1 mM (up triangles) and 0.6 mM (down triangles). The data shown are averages of the H8 and H2 line widths. The addition of 41 nmol of BKA after ATR titration in the presence of 1 mM AMP−PCP led to further line narrowing (indicated by the arrow).

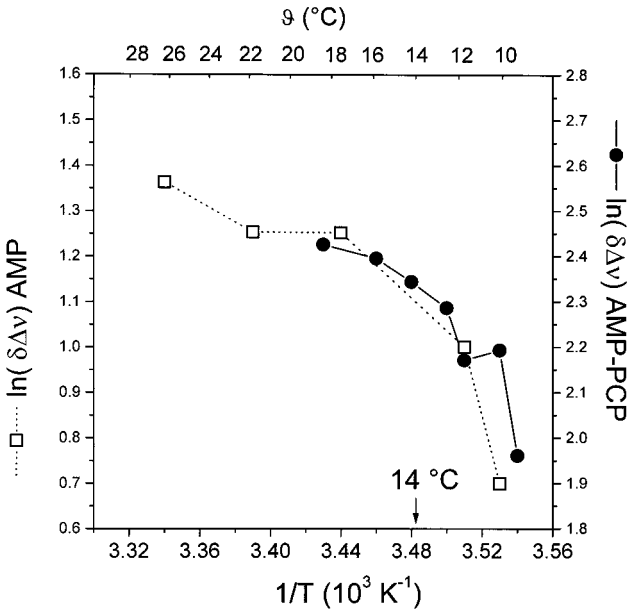

FIGURE 3: Temperature dependence of $\delta\Delta\nu$ for AMP (open symbols) and AMP−PCP (closed symbols). Approximately 20 mg/mL of mitochondrial protein: nucleotide concentration, 1 mM.

instead of CAT permits the rearrangement of the carrier from the c- into the m-state by addition of BKA at the end of the titration (*13*). The BKA-induced transition into the m-state elicits a further decrease of the nucleotide line width (insert in Figure 2).

An estimate of the off rate constant k_{off} for AMP−PCP binding at the c-site of the carrier can be obtained from the same data set according to

$$1/T_2^{obs} = (1 - p_b)/T_2^{f} + p_b/(T_2^{b} + k_{off}^{-1}) \qquad (1)$$

where p_b denotes the fraction of carrier bound nucleotide (*14*). The transverse relaxation time T_2^b refers to bound AMP−PCP, while T_2^{obs} and T_2^f are the relaxation times observed before and after CAT titration, respectively. The bound fraction, p_b, can be identified with the number of substrate binding sites as determined above (1.2 nmol/mg of mitochondrial protein), providing that the binding sites are saturated. The latter assumption is borne out by the total AMP−PCP concentration of 5 mM. Assuming that $T_2^b \ll k_{off}^{-1}$, the off-rate constant can be estimated

$$\Delta\nu_{obs} - (1 - p_b)\Delta\nu_f \approx p_b k_{off}/\pi \qquad (2)$$

where the proton line widths without and with CAT addition are denoted by $\Delta\nu_{obs}$ ($= 1/\pi T_2^{obs}$) and $\Delta\nu_f$, respectively. An evaluation according to eqs 1 and 2 of the data shown in Figure 2 yields an apparent $k_{off} \approx 2600\ s^{-1}$. The assumption of T_2^b being negligible may be not strictly applicable as somewhat different line broadenings, $\Delta\nu$, were observed for H8 and H2, respectively. Therefore, of course, the above calculation can only yield a lower limit value for k_{off}.

Effect of Temperature and Surface Charge. The temperature dependence of the difference of the line width, $\delta\Delta\nu$, obtained with and without CAT addition was studied using AMP and AMP−PCP which were chosen for their stability against ATPase activity during the course of the experiment (Figure 3). It can be recognized that the slope of $\ln(\delta\Delta\nu)$ vs $1/T$ changes between 13 and 15 °C, suggesting that there is a change of an activated process within this temperature range, most probably the release of the nucleotides from the binding site. Earlier reports on transport (*4*) and channel activity (*15*) of the carrier revealed a similar change of the activation energy at 14 °C. This temperature dependence indicates that a sample temperature >15 °C will be necessary for an accurate comparison of the of line broadenings (see below), considering the relative uncertainty of the NMR temperature control (±0.5 °C).

The dependence of $\delta\Delta\nu$ on surface charges was examined by mixing KCl and sucrose in the suspending buffer so as to keep the overall osmolarity of the medium constant. With sucrose alone, $\delta\Delta\nu$ was negligible and increased with increasing ionic strength (Figure 4). It can be concluded that screening of *negative* membrane surface charges results in decreasing electrostatic repulsion of the nucleotides which leads to increasing p_b (6). A comparison of the absolute line widths ($\Delta\nu$) with and without CAT (dotted lines in Figure 5) further suggests that the surface charge screening almost exclusively affects the binding to the c-site of the AAC rather than to other binding sites.

Selectivity of the c-Site for Nucleotide Binding. In exploratory experiments (*14*) various nucleotides, including mono-, di-, and triphosphates of purines and pyrimidines, were tested for CAT competition. Nucleotides such as ITP, GTP, and AMP which are translocated with very low or negligible activity (*16*, *17*) were nevertheless transiently bound at the

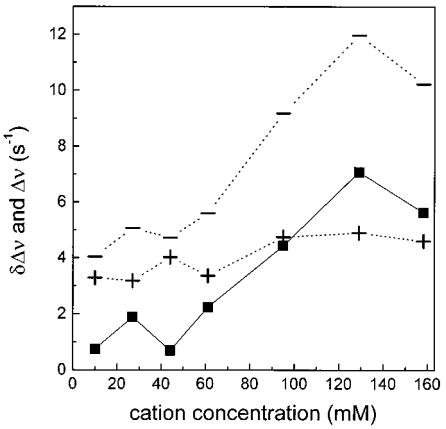

FIGURE 4: Variation of the ionic strength by changing the proportion of KCl and sucrose so as to maintain constant osmotic pressure. Mitochondria and nucleotide concentrations are as in Figure 3. The total cation concentration is given in the abscissa as a measure of the ionic strenght. AMP line widths without and with CAT are denoted by minus and plus symbols and the difference, $\delta\Delta\nu$, by solid squares, respectively. Error of line width measurement is as in Figure 2. Error bars are omitted for clarity.

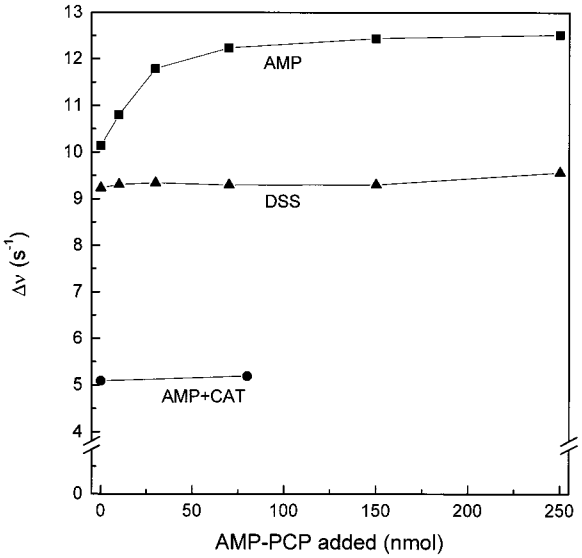

FIGURE 5: Effect of low AMP−PCP concentrations on the line width difference $\delta\Delta\nu$ of AMP (squares). Upon addition of >250 nmol of AMP−PCP, $\delta\Delta\nu$ again decreased due to competition (not shown). The absolute line widths, $\Delta\nu$, of the internal standard DSS (triangles) and of AMP (circles) *after* CAT addition are included. Note that the DSS line width, which probably reflects hydrophobic membrane interaction, was independent of CAT or nucleotide addition: concentrations of AMP and DSS, 1 mM; mitochondrial protein density, 15 mg/mL. Error of line width measurement is as in Figure 2. Error bars are omitted for clarity.

cytosolic site of the carrier as indicated by the line narrowing after CAT addition. These competition experiments were carried out at 12 °C in the presence of the ATPase inhibitor aurovertin B (10 nmol/mg of mitochondrial protein), and the mitochondrial density and nucleotide concentration were high enough to give an acceptable signal-to-noise ratio within a few minutes, thereby preventing degradation of the nucleotide di- and triphosphates by ATPase or adenylate kinase activities in the mitochondrial suspension. This protocol does not account, however, for the temperature dependence of the nucleotide−AAC interaction as shown above and for the different electrostatics of mono-, di-, and triphosphates with the membrane and protein surface charges. Therefore, to bring the structure−affinity relationship with respect to the nucleotide base moieties into focus, nucleotide monophosphates were studied at 18 °C in a buffer containing 150 mM KCl. This reduces the temperature sensitivity of $\delta\Delta\nu$ (Figure 3) and overcomes the problem of surface charge repulsion (cf. Figure 4).

Two additional improvements led to a much better confidence of the line width determinations and furnished the experimental conditions for an accurate distinction of small differences with respect to the nucleotide base structures. First, $\delta\Delta\nu$ was enhanced by the addition of 0.1 mM AMP−PCP (in the presence of 1 mM nucleotide monophosphate under study) in order to catalyze the c−m transition. At this concentration AMP−PCP mobilizes carrier sites for nucleotide monophosphate binding whereas competition is still negligible. This was confirmed in a separate experiment where it was shown that 0.25 mM AMP−PCP elicits an increase of $\delta\Delta\nu$ in the AMP spectrum by 15−20% (Figure 5), while larger concentrations lead to line narrowing by competition, as expected (not shown in Figure 5). Second, high resolution and sensitivity were achieved by sample spinning with digital sideband removal (see Methods) which made it possible to reduce the mitochondrial protein density to 20 mg/mL. With sample spinning and full line shape simulation line broadenings were typically determined with an error of less than 0.5 Hz.

A mitochondrial suspension was devided into 9 identical 0.8 mL samples, and the nucleotide monophosphates (including base structures with very different distributions of the electrostatic potential, cf. Figure 8), AMP−PCP, and the inhibitor CAT were added to final concentrations of 1 mM, 0.1 mM, and 133μM, respectively. This nucleotide concentration gave an approximately 40-fold molar excess over the AAC binding sites in the suspension. The results summarized in Figure 6 indicate that the presence of a purine ring is a necessary but not a sufficient condition for binding. Rather, only substitutions in position 6 of the purine moiety are compatible with proper binding site recognition. Binding may be also sensitive to the distribution of the molecular electrostatic potential (see Discussion).

The nucleotides in Figure 6 differ by their base or ribose structures. Recently, it has been shown that caged adenine nucleotides (caged ADP and caged ATP) which are photochemically hydrolyzed to yield ADP or ATP in situ partially inhibit the AAC catalyzed transport of ADP and ATP (*18*). Following a simple competition model (*19*) it can be expected that $\delta\Delta\nu^{-1}$ depends linearily on the total concentration of the competing ligand, $[I]_0$ (the caged compound):

$$\delta\Delta\nu_0/\delta\Delta\nu \propto ([I]_0/[L]_0)(K_d/K_I) \qquad (3)$$

which yields the ratio K_d/K_I of binding affinities of substrate and competitor ($\delta\Delta\nu_0$, CAT difference line broadening without caged nucleotide; $[L]_0$, concentration of AMP−PCP). A linear regression according to eq 3 (not shown) indeed revealed the competition at the c-binding site between the caged nucleotides and the nonhydrolyzable ATP analogue AMP−PCP (1 mM), that is, K_d/K_I was 37 ± 17 and 19 ± 4 for caged ADP and caged ATP, respectively, indicating that K_I is smaller for caged ADP than for caged ATP. This observation is in line with the earlier report on transport inhibition by the caged compounds (*18*). Irradiation of the

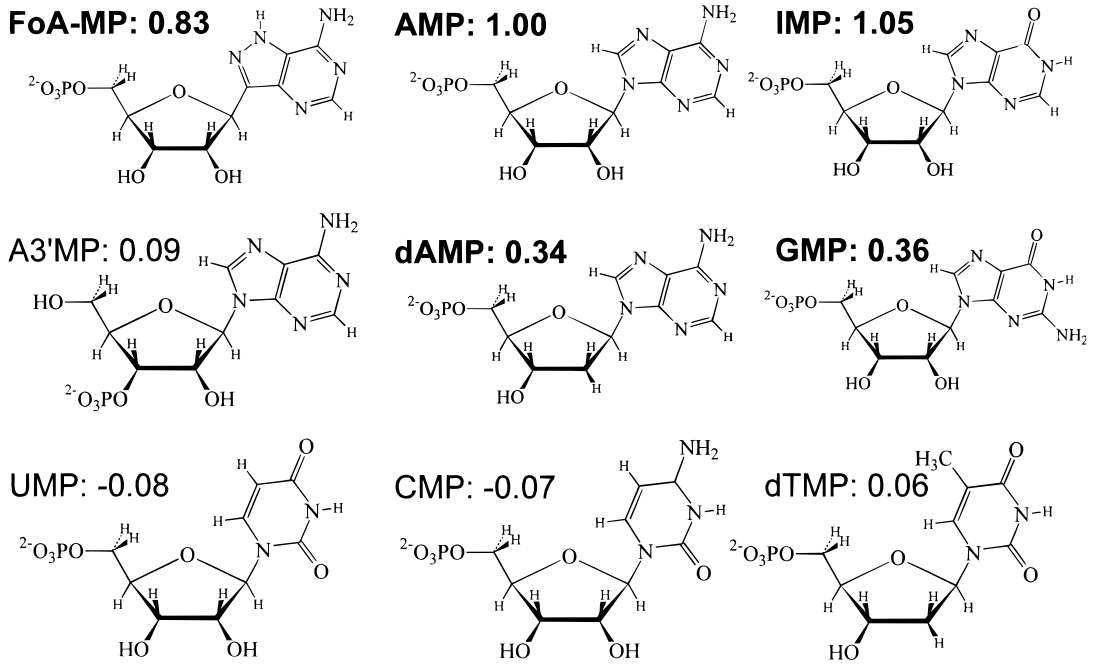

FIGURE 6: Relative affinities of nucleotide monophosphates. The inhibitor difference, $\delta\Delta\nu$, is arbitrarily set to 1.00 for AMP. Bold lettering is to emphasize high affinity for the AAC.

samples after addition of the caged nucleotides at 366 nm (3 min) led to a significant decrease of $\delta\Delta\nu_0/\delta\Delta\nu$, corresponding to approximate K_d/K_I ratios of 7 and 4, respectively, for photolytically liberated ADP and ATP. Thus, the caged nucleotides are more tightly bound in the carrier binding site than the ordinary substrate molecules.

Conformation of the Transiently Bound Nucleotides. Intramolecular cross relaxation in a ligand bound to a macromolecule can be utilized for measurements of internuclear distances, provided that the ligand exchange between binding site and bulk solution is rapid relative to the spin−lattice relaxation rate of the bound ligand. The k_{off} rate as determined above (eq 2) and the size of the mitochondria meet the requirements for an assessment of the nucleotide conformation by the transferred nuclear overhauser effect (TRNOE). Selective inversion of an exchange averaged ligand resonance then results in a TRNOE on adjacent nuclei. A band selective shaped pulse (half gauss) was applied for signal inversion which avoids indirect protein−ligand magnetization transfer by spin diffusion (*19*, *20*). Measurements were performed at an appoximately 400-fold molar excess of AMP−PCP over the carrier binding sites. Again, competition with CAT served as a control. The normalized TRNOE values for a number of spin pairs are shown in Table 1. The H4'-H1' proton pair was chosen for normalization and distance calculation. The distance of this pair is 4.0 Å, irrespective of the ribose ring pucker conformation. The AMP−PCP conformation derived from the TRNOE data is shown in Figure 7. The strong TRNOE obtained for H5',5''-H8 and H3'-H8 indicate that the nucleotide assumes an anti conformation of the carrier bound state while the sizable effects between the β,γ-CH_2 protons and H8, H2, and H1', respectively, led to the conclusion that the triphosphate moiety bends toward the purine ring as shown in Figure 7.

The TRNOE was only partially suppressed by CAT, indicating that there is still some weak binding of the nucleotide. The TRNOE obtained with CAT was not due to nonspecific membrane binding as denaturation by incubation of the suspension at 80 °C for 5 min led to complete disappearance of the effect. Moreover, an analogous experiment performed with the membrane reconstituted carrier (not shown) gave very similar results.

Table 1: Normalized[a] TRNOE

proton pair	without CAT	with CAT
H5′,5″−H8	1.13	0.53
H5′,5″−H2	0.20	0.12
H5′,5″−H1′	0.75	0.46
H4′−H8	0.66	0.21
H4′−H1′	1.00	0.64
H3′−H8	0.75	0.46
H3′−H1′	0.44	0.16
H1′−H8	0.48	0.21
H1′−H2	0.25	0.20
$\beta,\gamma CH_2$−H8	0.18	nd
$\beta,\gamma CH_2$−H2	0.20	nd
$\beta,\gamma CH_2$−H1′	0.22	nd
H2−H1′	0.33	nd
H8−H1′	0.66	0.33

[a] All values normalized with respect to H4′−H1′ (H4′ selectively inverted). The absolute TRNOE was −6.4% for this proton pair.

DISCUSSION

Selectivity for ATP and ADP transport is a salient feature of the mitochondrial ADP/ATP carrier (*16*). Some transport activity, ranging between 10% and 20% of that obtained with ADP, was found for AMP−PCP and AMP−PNP and for formycin-A diphosphate in rat liver mitochondria (*21*). Small transport activities were also reported for the 2′-deoxy analogues of ADP and ATP (*22*). Other purine and pyrimidine nucleotide di- and triphosphates, however, are excluded from translocation. A general concept of carrier catalysis was derived from extensive data on ligand interaction with the AAC, that is, binding of substrates, substrate analogues, and specific inhibitors (*23*). It was assumed that the large energy required for the conformational transition that accompanies

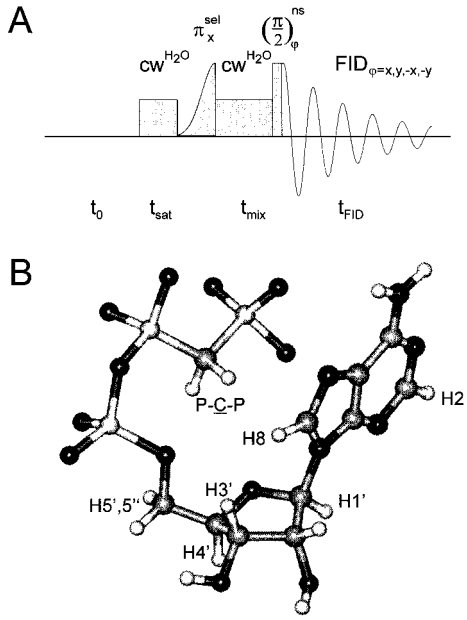

FIGURE 7: (A) Selective signal inversion pulse sequence for TRNOE measurements: preacquisition delay (t_0), 0.1 s; saturation time (t_{sat}), 0.5 s; mixing time (t_{mix}), 0.125 s; acquisition time (t_{FID}), 0.82 s. Presaturation was performed at low power ($\gamma B_2/2\pi = 330$ Hz). (B) Molecular model derived from the inhibitor difference TRNOE by distance calculations using the H4′−H1′ proton pair for calibration (Table 1). The calibration distance of 4.0 Å was taken from a molecular model. The aproximate error of the signal integrals was ±20% which translates into an absolute error of the interproton distance values of ±0.2 Å. The structural model was obtained by simulated annealing using the TRNOE derived distances as constraints. The maximum error between the experimental values and the structure shown was 0.5 Å.

the translocation step is coupled to the energy of substrate binding (*24*). This hypothesis is strongly supported by the observation that in the absence of substrates the carrier is locked in either of the two conformational states (*16*). The negligible transport of AMP (vs ATP and ADP) hints to the importance of an electrostatic energy input for the carrier transition; that is, the two negative net charges of the nucleotide monophosphate may not suffice to induce the transition state. As shown here, however, AMP is recognized at the cytosolic binding site of the AAC, suggesting that substrate *recognition* and *translocation* are distinct steps in the carrier pathway.

The present study aims at an understanding of substrate recognition in the c-binding site of the carrier. An NMR measurement of nucleotide binding (as opposed to translocation) in a well-defined conformational state is not a trivial task. A maximum number of carrier sites should be available for the binding of the nucleotides under study. Moreover, the nucleotides must not be hydrolyzed within the time range of the experiment. The first goal was achieved by addition of a small amount of the noncleavable analogue AMP−PCP which elicits a maximal $\delta\Delta\nu$ as shown in Figure 5. This may be due to the accumulation of c-binding sites on the cytosolic surface of the inner membrane or to an induced fit effect by AMP−PCP. Nucleotide monophosphates were employed in order to comply with the second condition. The exclusion of the monophosphates from translocation represents an additional advantage here as this warrants that the observed ^{1}H-line broadening is due to transient binding in

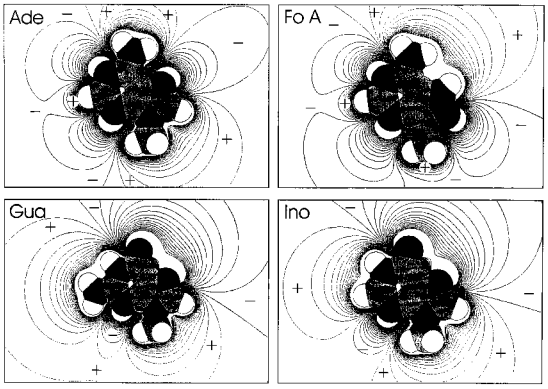

FIGURE 8: Electrostatic potential distribution in methylated (at N-9 or C-9) nucleobases: Ade, N-9-methyl adenine; FoA, C-9-methyl formycin; Gua, N-9-methyl guanine; Ino, N-9-methyl inosine. Geometry optimization and calculation of electron density was performed by a semiempirical MO method (PM3). A grid in the molecular plain of 128 × 128 grid points and 33 contour levels was employed. The electrostatic potential is shown from −0.0825 esu to +0.0825 esu with a step size of 0.005 esu. The size of the atoms corresponds to standard van der Waals radii: carbons, gray; nitrogenes, black; hydrogenes, white.

the c-site rather than to a contribution of the transition state of the translocation.

To establish a structure−affinity relationship with respect to the nucleotide bases it is also advantageous to compare nucleotide monophosphates (Figure 6). The structural prerequisites for substrate recognition in the c-binding site of the AAC can thus be delineated, providing that the ^{1}H-line broadenings are determined with an accuracy of less than 1 Hz. This was achieved by sample spinning and digital sideband removal (see Methods). The results shown in Figure 6 highlight the role of structural details in the nucleotide base and in the ribose moiety for the recognition in the cytosolic binding site of the AAC. The carrier obviously rejects the pyrimidine nucleotides and purine nucleotide monophosphates other than the 5′-derivatives, for example, adenosine-3′-monophosphate. Binding of 3′,5′-cyclic AMP, which has only one net negative charge, was also negligible (not shown in Figure 6). The reduced effect obtained with d-AMP reveals the significance of the 2′-OH group for substrate recognition, in analogy with the low transport activity observed for the 2′-deoxy derivatives of ATP and ADP (*16*). Likewise, the low affinity of GMP indicates that an amino group in position 2 of the purine ring is not compatible with proper c-state binding. This is in agreement with the exclusion of the guanosine nucleotides from translocation (*4*). Even the isomerism of formycin versus adenine (positional exchange of C-8 and N-9), which preserves the planar ring structure, interferes with the recognition in the c-binding site.

This renders the binding of IMP somewhat unexpected as the replacement of the amino group in AMP with an oxo group will certainly alter the charge distribution and the distribution of the electrostatic potential. Therefore, molecular isopotential surfaces were calculated for the methylated purine bases (N-9-methyl adenine, N-9-methyl hypoxanthine, N-9-methyl guanine, and the C-9 methyl derivative of formycin-A; cf. Figure 8) in order to visualize the effect of changing the purine ring structure and to appreciate the aptitude of the respective intramolecular charge distributions for c-site binding. The structures of AMP, IMP, and

formycin-A monophosphate can be regarded as "bioisosteric" (*25*). The different affinities then underscore the importance of the intramolecular electrostatics for proper binding site recognition. The potential distribution is quite similar, however, for the IMP (as shown by *N*-9-methyl hypoxanthin in Figure 8) and GMP ring moieties, which differ significantly in this regard from adenine and formycin. Thus, it must be concluded that the low affinity of GMP versus IMP is due to steric hindrance by the amino group in the 2-position of the purine ring rather than to the details of the isopotential surfaces.

An analogous calculation of electrostatic potentials has been recently performed for an understanding of the competition between ATP and GTP and the fluorescein derivative eosine Y in the m-state of the AAC (*26*). In contrast to ADP and ATP, GTP was unable to displace eosin Y which was attributed to the different electrostatics of the nucleotides. Considering the relative affinity of IMP, however, it is more likely that this is due to the guanine amino group rather than to the different electrostatics.

The 1-(2-nitrophenyl)ethyl esters of ADP and ATP (caged ADP or ATP) have long been utilized for the sudden photochemical release of the nucleotides in situ (*27*, *28*). The caged compounds, while not being translocated by the AAC, interfere with the transport of free nucleotides (*18*). The present results provide more direct evidence for the competition between caged and free nucleotides in the cytosolic AAC binding site. The approximate ratio of the K_I values for caged ADP and caged ATP as calculated from eq 3 is 0.5 which may be compared to the K_I ratio of 0.3 observed previously for transport inhibition (*18*). Thus, in the AAC binding site the nitrophenyl residue seems to furnish a considerable binding contribution which probably makes the effective ATP or ADP concentration after photolysis in the binding site different from the calculated total nucleotide concentration.

The inhibitor sensitive NMR line broadening of added nucleotides indicates that the on/off exchange in the binding site is faster than the translocation rate. This is borne out by the off rate constant of AMP−PCP, $k_{off} \approx 2600\ s^{-1}$, which was obtained at 18 °C as an estimate from Figure 2. This rate is approximately 6000 times larger than the expected translocation rate for AMP−PCP (i.e., v_{max}/E_0) at 18 °C (*5*, *16*). It may be noted that a similar titration with ATP (not shown) which was performed at 12 °C (in order to reduce the rate of ATP hydrolysis) yielded $k_{off} \approx 500\ s^{-1}$ (*14*). Considering the simplifying assumption $T_2^b \ll k_{off}^{-1}$, the true k_{off} values may be even larger than this.

It must be emphasized that the surface charges contributed by negatively charged membrane phospholipids and positively charged amino acid residues in the AAC required a well-defined and constant ionic strength throughout the titrations if the determination of the inhibitor difference line broadening was to be meaningful. Variation of the ionic strength indeed affects the affinity of nucleotides as shown in Figure 4, suggesting that electrostatic repulsion prevents the negatively charged nucleotides from approaching the membrane surface. A strong interaction of the negatively charged phospholipid cardiolipin with the detergent solubilized AAC has been previously demonstrated by NMR and ESR spectroscopy (*29*−*31*). A predominance of cardiolipin in the phospholipid boundary layer of the AAC can be expected to result in repulsion of the nucleotides when there is no or insufficient charge screening.

Scheme 1

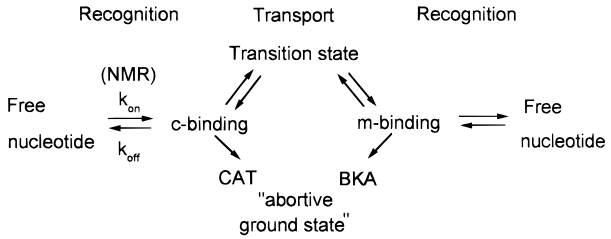

A single break around 14 °C was detected in the temperature dependence of nucleotide transport in mitochondria, in reconstituted preparations of the AAC, and in a study that revealed the channel activty of the carrier (*1*, *18*, *32*). In bovine heart mitochondria, activation energies of 143 and 63 kJ/mol were obtained below and above the break temperature, respectively. A break can be also recognized in the temperature dependence of $\delta\Delta\nu$ (Figure 5) where a tentative calculation yields activation energies of 60 and 10 kJ/mol, respectively. Aside from the relative uncertainty of the present activation energy calculation, it can be concluded that the temperature dependence of $\delta\Delta\nu$ is a property of the protein rather than of the surrounding lipids, in agreement with the earlier reports on substrate transport. Considering the close similarity of the temperature dependence for nucleotide transport and binding it may be argued that there is a thermal threshold where the carrier protein becomes more malleable for the induced fit of the substrate into the binding pocket *and* for the propagation into the transition state.

It is generally recognized that the ADP/ATP carrier protein functions as a homodimer. This raises the question as to the number of nucleotide binding sites per dimer. The presence of a low-affinity binding site was deduced from titrations with radioactive [^{35}S]-CAT (*23*) and from an electron spin resonance study using a spin-labeled derivative of CAT (*33*). While these earlier observations refer to inhibitor binding, the present results also provide evidence for more than one *substrate* binding site in the c-state. The sigmoidal curve obtained with ATR may be attributed to competition about a weak binding site in the c-conformation of the carrier. Rearrangement into the m-state by BKA abolishes this weak interaction and results in further line narrowing (insert in Figure 2). The significant TRNOE observed after CAT addition may be also due to a weak residual interaction with the c-site. These observations are in line with a report on the anion dependence of the reconstituted carrier activity where it was shown that the adenine nucleotide transport is stimulated by small anions and nucleotides with an apparent Hill coefficient $n = 2$ (*7*). The same study revealed a competetive inhibition of the adenine nucleotide transport by anions. Most notably, the ratio of stimulatory and inhibitory effects was larger by orders of magnitude for ATP than for GTP or inorganic anions.

In summary, it can be concluded that nucleotide translocation by the AAC entails distinct steps as outlined in Scheme 1. The first step, nucleotide recognition, is less selective than the translocation step, as revealed by accurate NMR line width determinations using the inhibitor difference method. A purine base without a bulky substituent at C-2 is a minimal condition for c-state binding, irrespective of the number of phosphate residues. The electrostatic interaction of the di- and triphosphates with the AAC provides the

additional energy for the translocation step, whereas the AAC−inhibitor complex represents a low-energy trap (*34*, *35*) (Scheme 1). In the c-state binding the nucleotides assume an anti conformation. At the same time the observed magnetization transfer between the β,γ-methylene bridge and adenine and ribose protons of AMP−PCP suggests a backfolded conformation of the β,γ-methylene triphosphate moiety. Finally, binding of nucleoside diphosphates and nucleoside triphosphates seems to mobilize the otherwise rigid AAC which allows for enhanced binding of the more weakly interacting monophosphates (Figure 3) or for the transition into the translocation path. It remains to be elucidated how the thermal transition observed for binding and transport is related to the induced fit that eventually results in nucleotide translocation.

ACKNOWLEDGMENT

The excellent technical assistance of Brigitte Nuscher is gratefully acknowledged.

REFERENCES

1. Aquila, H., Link, T. A., and Klingenberg, M. (1987) *FEBS Lett. 212*, 1−9.
2. Palmieri, F., Indiveri, C., Bisaccia, F., and Krämer, R. (1993) *J. Bioenerg. Biomembr. 25* (5), 525−535.
3. Klingenberg, M. (1972) in *Mitochondria Biomembranes*, pp 147−162, Elsevier, Amsterdam, The Netherlands.
4. Weidemann, M. J., Erdelt, H., and Klingenberg, M. (1970) *Eur. J. Biochem. 16*, 313−335.
5. Klingenberg, M., Grebe, K., and Appel, M. (1982) *Eur. J. Biochem. 126*, 263−269.
6. Krämer, R. (1983) *Biochim. Biophys. Acta 735*, 145−159.
7. Krämer, R., and Kürzinger, G. (1984) *Biochim. Biophys. Acta 765*, 353−362.
8. de Brujjn, J., Frost, D. J., and Nusteren, D. H. (1973*) Tetrahedron Lett. 29*, 1541−1547
9. Blair, P. V. (1967) *Methods Enzymol. 10*, 78−81.
10. Geen, H., and Freeman, R. (1991) *J. Magn. Reson. 93*, 93−141.
11. Klingenberg, M., Riccio, P., and Aquila, H. (1978) *Biochim. Biophys. Acta 503*, 193−210.
12. Klingenberg, M., Appel, M., Babel, W., and Aquila, H. (1983) *Eur. J. Biochem. 131*, 647−654.
13. Klingenberg, M. (1976) *Enzymes Biol. Membr. 3*, 383−438.
14. Stöckl A. (1995) Ph.D. Thesis, Technische Universität München, Munich, Germany.
15. Broustovetsky, N., and Klingenberg, M. (1996*) Biochemistry 35*, 8483−8488.
16. Klingenberg, M. (1985) *Enzymes Biol. Membr. 4*, 511−553.
17. Pfaff, E., and Klingenberg, M. (1968) *Eur. J. Biochem. 6*, 66−79.
18. Broustovetsky, N., Bamberg, E., Gropp, T., and Klingenberg, M. (1997) *Biochemistry 36*, 13865−13872.
19. Ni, F. (1994) *Prog. Nucl. Mag. Reson. Spectrosc. 26*, 517−606.
20. Clore, G. M., and Gronenborn, A. M. (1983) *J. Magn. Reson. 53*, 423−442.
21. Klingenberg, M. (1974) in *Dynamics of Energy-Transducing Membranes* (Estabrook R. W., Slater E. C., Eds.) pp 229−243, Elsevier Scientific Publishing Co., Amsterdam, The Netherlands.
22. Pfaff, E. (1967) in *Mitochondrial structure and compartmentation* (Quagliariello, E., Papa, S., Slater, E. C., and Tager, J. M., Eds.) pp 305−307, Bari, Adraiatica Editrice.
23. Klingenberg, M., Grebe, K., and Scherer, B. (1975) *Eur. J. Biochem. 52*, 351−363.
24. Klingenberg, M. (1989) *Arch. Biochem. Biophys. 270*, 1−14.
25. Silverman, R. B. (1992) *The organic chemistry of drug design and drug action*, Academic Press, London, U.K.
26. Majima, E., Yamaguchi, N., Chuman, H., Shinohara, Y., Ishida, M., Goto, S., and Terada, H. (1998) *Biochemistry 37*, 424−432.
27. McCray, J. A., Herbette, L., and Trentham, D. R. (1980) *Proc. Natl. Acad. Sci. U.S.A. 77*, 7237−7241.
28. Hibberd, M. G., and Trentham, D. R. (1986) *Annu. Rev. Biophys. Biophys. Chem. 15*, 119−161.
29. Beyer, K., and Klingenberg, M. (1985) *Biochemistry 24*, 3821−3826.
30. Drees, M., and Beyer, K. (1988) *Biochemistry 27*, 8584−8591.
31. Hoffmann, B., Stöckl, A., Schlame, M., Beyer, K., and Klingenberg, M. (1994) *J. Biol. Chem. 269*, 1940−1944.
32. Krämer, R., and Klingenberg, M. (1982) *Biochemistry 21*, 1082−1089.
33. Munding, A., Beyer, K., and Klingenberg, M. (1983) *Biochemistry 22*, 1941−1947.
34. Klingenberg, M. (1989) *Methods Enzymol. 171*, 12−32.
35. Dawson, A., Klingenberg, M., and Krämer, R. (1987) in *Mitochondria − a practical approach*, (Darley-Usmar, V. M., Rickwood, D., and Wilson, M. T., Eds.) pp 35−78, IRL Press, Oxford/Washington, D.C.

BI981431L